Two-Electron Photodetachment of Negative Ions in a Strong Laser Field

Boris Bergues and Igor Yu. Kiyan

Physikalisches Institut, Albert-Ludwigs-Universität, D-79104 Freiburg, Germany

(Received 8 January 2008; published 11 April 2008)

We study the photodetachment of H^-, F^-, and Br^- in a short laser pulse of 800 nm wavelength and 6×10^{14} W/cm^2 peak intensity. Photoelectron spectra, recorded with the use of an imaging technique, reveal a substantial contribution from the sequential process of double detachment of halogen negative ions. The saturation effect is shown to play a crucial role in this process. The role of the alignment of atoms produced by photodetachment is discussed.

DOI: 10.1103/PhysRevLett.100.143004 PACS numbers: 32.80.Gc, 32.80.Rm

Multiple electron ionization of atoms in a strong laser field has received much attention over the past years. A wide discussion was devoted to the mechanism of this process. Earlier studies on double ionization of alkaline earth atoms in a laser field of 10^{11}–10^{13} W/cm^2 intensity revealed the sequential ionization to be the dominant mechanism in the production of doubly charged positive ions [1]. It was shown that in the first stage of the sequential process singly charged ions are formed in excited states, which are subsequently ionized in the second stage. The importance of electron correlations was pointed out. In later experiments the multiple ionization was studied in noble gases at higher intensities reaching the value of 10^{16} W/cm^2 [2]. A striking feature discovered in these studies is the presence of a ''knee'' in the yield curve of multiply charged ions as a function of laser intensity [3]. At intensities below the knee value multiple ionization has a nonsequential character, as is shown by the *S*-matrix calculations [4] where electron correlations are taken into account. The latest experiments that involve the measurement of the recoil momentum of ions appear to land additional support [5,6]. Several models were proposed to describe the nonsequential ionization mechanism. Among these is the rescattering model [7], which describes well the latest data on Ne [6] while other mechanisms can be ruled out. Such a conclusion, however, cannot be drawn clearly from the data on He and Ar [5]. In general, multiple ionization represents a process of correlated multielectron dynamics and can involve a complicated interplay between sequential and nonsequential pathways, as was recently demonstrated in Ref. [8].

While multiple ionization of atoms has been under consideration for many years, multiple detachment of atomic negative ions in a strong laser field is essentially unexplored and, thus, represents a novel and interesting subject. The different character of binding forces and the enhanced role of electron correlations in negative ions, as compared to atoms, bring a variety in the conditions that determine the mechanism of multielectron emission. The goal of the present Letter is to reveal the mechanism of double detachment. As will be shown below, the ratio between the ionization potential and the electron affinity of the parent atom is the essential parameter that governs this process. For different elements of the periodic table this ratio varies in a rather wide range. For example, its value is approximately 3.5 for Br, 5 for F, and 18 for H. In the present Letter we consider double detachment of negative ions of these three elements. For comparison, a typical ratio of the second and first ionization potentials of alkaline earth and noble gas atoms is approximately 2.

The study of multiple detachment of negative ions includes, to our knowledge, only a few experiments, where only the total yield of generated positive ions was measured as a function of laser intensity [9,10]. In Ref. [9] the yield was recorded at the saturation threshold of double detachment under a relatively long pulse regime of 170 ps, where the sequential mechanism should be expected. A counterintuitive behavior of saturation intensities for some target ions was reported there. In particular, double detachment of Ag^- is found to be easier to saturate than double detachment of Al^-, though both the electron affinity and the ionization potential of Ag are greater than those for Al. This surprising result is interpreted in Ref. [11] by considering the alignment of the residual atoms in the first step of the sequential process and the m dependence of the ionization rate in the second step. The relevance of the alignment effect in the present study will be discussed.

As an alternative approach to the study of double detachment, we employ an electron imaging technique to measure the angle resolved momentum distributions of photoelectrons. Measurements are performed on Br^-, F^-, and H^- with a linearly polarized laser beam of 800 nm wavelength and 100 fs pulse duration. By using different target ions we aim to investigate the process of two-electron detachment in dependency on the type of the parent atom. The minimum number of photons needed to overcome the unperturbed detachment threshold is three for the halogen negative ions and one for H^-.

Our experimental setup is described elsewhere [12]. Briefly, a mass-selected beam of negative ions is intersected with the laser beam inside an electron imaging spectrometer, where the detached electrons are projected by means of an electrostatic field onto a calibrated position sensitive detector. The image processing involves a con-

ventional Abel inversion routine, which reconstructs the angle resolved momentum distribution of photoelectrons emitted from the laser focus. The signal in the reconstructed images has a dynamic range of approximately 3 orders of magnitude. The laser beam is delivered from a Ti:sapphire laser system operating at a repetition rate of 1 kHz. A typical focus size of 30 μm and a pulse duration of 100 fs are measured with the use of our beam diagnostic tools. The peak intensity in the focus is of the order of 6×10^{14} W/cm^2, though its value slightly varies for different measurements.

The measured angle resolved momentum distribution of photoelectrons emitted from Br^- is shown in Fig. 1(a). At low momenta the distribution consists of a few ponderomotively broadened excess photon detachment (EPD) peaks. In our previous studies [12], we have proved that the theory by Gribakin and Kuchiev [13] is rather reliable in the quantitative description of the photodetachment process. By performing simulations with the use of their predictions for the differential photodetachment rate, we find that the part of the spectrum at low momenta represents basically a contribution from the process of single electron detachment of Br^-. Details on the simulation routine can be found in [12]. The calculated spectrum is presented in Fig. 1(b). Indeed, it reproduces well the EPD

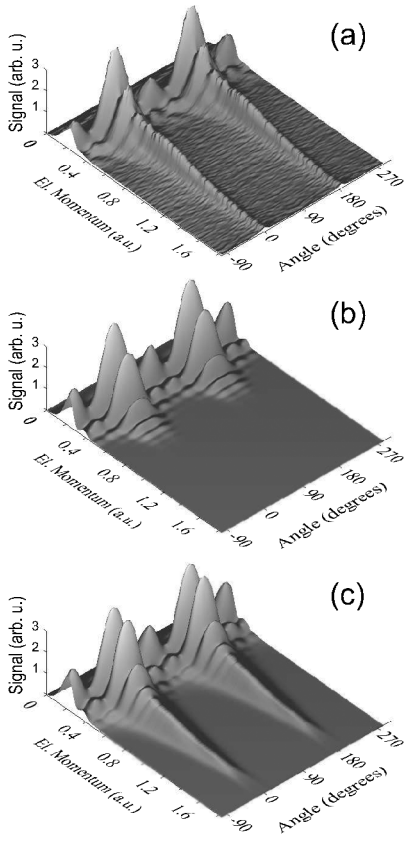

FIG. 1. Angle resolved momentum distribution of electrons detached from Br^-: (a) experimental spectrum, (b) simulated spectrum of single electron detachment, (c) simulated spectrum of sequential double detachment.

structure at low momenta. However, one can see that it fails to reproduce the well-pronounced jets pointing along the laser polarization direction at higher electron momenta. Since the height of the jets is only an order of magnitude lower than the maximum of the spectrum, it is unlikely that the origin of the jets is the rescattering effect. From another side, our calculations point to a strong saturation of the photodetachment process under the given experimental conditions. It means that negative ions are converted to atoms at the leading front of the laser pulse, and the atoms created this way represent a target for the main part of the pulse. Therefore, the contribution from the subsequent ionization process has to be considered.

In order to simulate the sequential double detachment, we solve the following system of rate equations to describe the evolution of a population of negative ions $N(r, t)$ and atoms $A(r, t)$ during the interaction with the laser pulse:

$$\begin{aligned} \dot{N} &= -N[2w_0^d(I) + 4w_1^d(I)], \\ \dot{A}_0 &= 2Nw_0^d(I) - A_0[w_0^i(I) + 4w_1^i(I)], \\ \dot{A}_1 &= 4Nw_1^d(I) - A_1[2w_0^i(I) + 3w_1^i(I)], \end{aligned} \tag{1}$$

with the initial conditions $N(r, -\infty) = 1$ and $A_{0,1}(r, -\infty) = 0$. Here $w_{0,1}^d$, $w_{0,1}^i$ denote the total rate of photodetachment and ionization from the $m = 0$ or $m = \pm 1$ initial state component, respectively, and $A_{0,1}$ represents the population of atoms having an $m = 0$ or $m = \pm 1$ hole in the closed p^6 outer shell. The laser polarization direction defines the angular momentum quantization axis. Thus, the atoms are considered to be aligned after the first step of the sequential process. The intensity distribution $I = I(r, t)$ is represented by a product of spatial and temporal Gaussian profiles with the experimental beam parameters given above. The photoelectron spectrum is obtained by integrating over space and time the differential rates for detachment and ionization weighted with the corresponding populations of negative ions and atoms, respectively, and by adding the detachment and ionization contributions together. The differential and total rates of both the detachment and ionization processes are calculated according to the analytical predictions derived in Ref. [13]. The theory used here is based on the strong-field approximation, where the core potential is neglected in the description of the continuum states of photoelectrons. Though this approximation is less accurate for the process of ionization, the Coulomb corrections are important at low electron momenta [14], where the signal is dominated by the process of photodetachment. The photoelectron distribution simulated for the sequential double detachment of Br^- is shown in Fig. 1(c). It describes well the shape of the experimental spectrum.

It should be pointed out that the detachment signal and the ionization signal appear quite separated on the momentum scale in the spectrum. This is due to the fact that the two steps of the sequential process are driven at rather different intensities. The detachment step is already saturated at the leading front of the pulse, where the intensity is

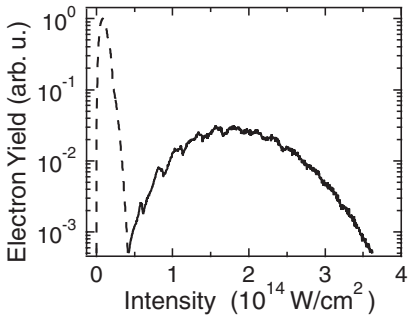

FIG. 2. Calculated intensity distribution of electrons emitted from Br^- in the detachment step (dashed line) and in the sequential ionization step (solid line). The focus geometry, the saturation effect, and the dynamic of populations of negative ions and atoms during the laser pulse are taken into account. The peak intensity in the focus is 6×10^{14} W/cm^2.

still insufficient for the ionization step. As an illustration, Fig. 2 shows simulated intensity distributions of the yield separately for the detachment and for the ionization step. The big difference in intensities needed to drive the two processes should be referred to a rather big ratio of 3.5 between the ionization potential and the electron affinity of Br (see the introductory section).

Our simulations reveal that not only the detachment step but also the ionization of Br atoms is saturated (also note that the ionization yield shown in Fig. 2 arises at intensities far below the peak intensity). One should refer at this point to the alignment effect that was taken into account. This effect leads to a reduction of the ionization rate. Indeed, in a linearly polarized field the detachment or ionization from the $m = 0$ component of the initial state represents the dominant contribution to the rate [15]. Hence, after the first step of the sequential process the aligned Br atoms posses only one electron with $m = 0$. Should relaxation of the alignment take place, the population of the $m = 0$ component of the $4p$ state would be $5/3$ times higher, and approximately so much higher would be the ionization rate. In the presence of saturation, the reduction of the ionization rate results in a modification of the shape of the photoelectron distribution. This is because atoms survive longer in the external field and, thus, can be exposed to higher intensities. Hence, the spectrum of ionized electrons extends to higher kinetic energies. In order to support this discussion we performed simulations, similar to those described above, where we allowed for relaxation of aligned Br atoms before the ionization step. Figure 3 shows a comparison between the two simulations and the experimental results. It demonstrates that the alignment effect does lead to an extension of the electron distribution to higher kinetic energies. However, this effect is not so significant in the shown spectrum. We expect the alignment effect to be much more pronounced for negative ions with an open shell containing only one electron with $m = 0$. In this case the ionization rate of an aligned atom would be defined only by the $m \neq 0$ components and would differ dramatically from the ionization rate of a nonaligned atom.

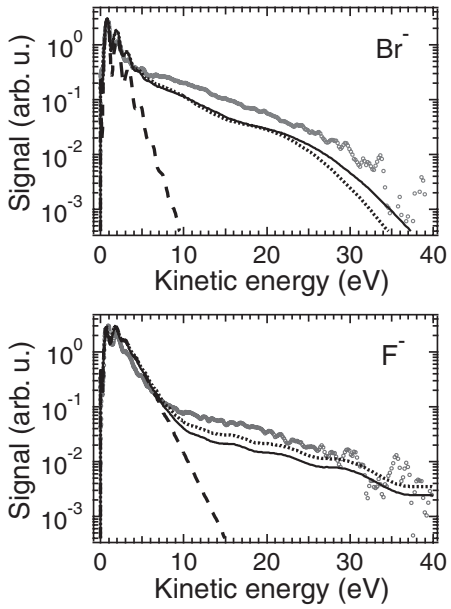

FIG. 3. Kinetic energy distribution of electrons detached from Br^- and F^- along the laser polarization axis. Circles represent experimental data. Solid and dotted curves show simulated spectra with and without taking the alignment effect into account. Dashed curves represent results of simulations where only single electron detachment is considered.

Experimental data obtained for F^- are also well described by the sequential model (see Fig. 4). Because of the higher ratio of the ionization potential to electron affinity of the F atom, the relative contribution to the signal from the ionization step is smaller, as manifested by the lower height of the jets in the spectrum (for a detailed comparison between spectra of F^- and Br^- see Fig. 3). The ionization potential of F is approximately by 5.6 eV higher than the ionization potential of Br. Therefore, ionization of

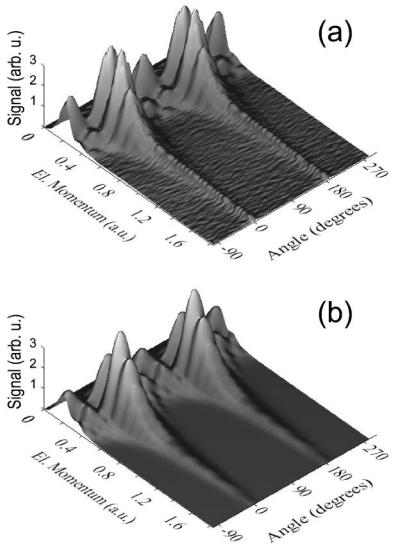

FIG. 4. Distribution of electrons detached from F^-: (a) experimental spectrum, (b) simulated spectrum of sequential double detachment.

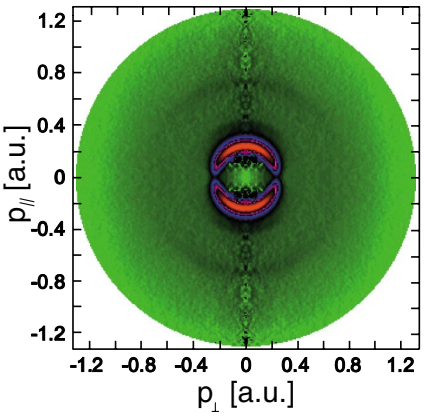

FIG. 5 (color online). Momentum distribution of electrons detached from H^-.

fluorine atoms is less saturated. It leads to an extension of the spectrum of ionized electrons to higher kinetic energies, as one can see from Fig. 3. This result is in accord with the discussion presented in the previous paragraph. Since ionization of F atoms is less saturated, the alignment effect results simply in a reduction of the ionization yield without modifications in the shape of the spectrum. The reduction factor is 1.43, which is close to the expected value of 5/3.

It should be noted that in the present calculations we do not take into account channels involving excitation of residual atoms after the first stage of the sequential process. Contribution of these channels might remove the remaining discrepancy between theory and experiment.

The measured momentum distribution of electrons detached from H^- is shown in Fig. 5 in the $(p_\parallel, p_\perp)$ coordinates, where $p_\parallel$ and $p_\perp$ denote the momentum components parallel and perpendicular to the laser polarization axis, respectively. One-photon detachment of H^- constitutes the dominant contribution to the spectrum, which appears as a ring of radius $p = 0.24$ a.u. with a characteristic p-wave angular modulation. Since the one-photon process strongly saturates the detachment step, the depletion of negative ions at the leading front of the laser pulse prevents observation of high-order EPD peaks. Only the first EPD peak, which corresponds to two-photon detachment, is slightly visible in the spectrum at a radius $p = 0.4$ a.u.. Despite the efficient conversion of negative ions to atoms, the contribution from the sequential ionization step is not visible in the spectrum. This is due to the limitation of the dynamic range of our apparatus specified above. Since detachment of H^- involves absorption of only one photon, the laser focus region where this process is saturated is much larger than the saturation region of higher-order detachment of halogen negative ions. Apart from the enlarged volume of signal acquisition, electrons detached from H^- contribute to a single narrow energy peak, instead of spreading over several broad EPD peaks. As a result, the maximum of the detachment signal is considerably enhanced and it exceeds the ionization signal by more than three orders of magnitude, which constitute the dynamic range of the signal.

It is interesting to point out that the distribution shown in Fig. 5 exhibits an additional structure consisting of a ring of radius $p = 0.75$ a.u., which corresponds to a kinetic energy of 7.7 eV. The origin of this structure is not yet understood and requires further investigations. We also hope that our finding will stimulate the development of more sophisticated theoretical approaches to the problem of strong-field photodetachment.

In conclusion, the process of double detachment of negative ions is studied for the first time with the method of electron imaging spectroscopy. We have shown that under the experimental conditions used here this process is governed essentially by a sequential mechanism. This fact is derived from the good agreement between experimental results and predictions by theory based on the strong-field approximation. Saturation plays a crucial role in the formation of photoelectron spectra. Because of saturation, the detachment and ionization steps are driven by quite different laser intensities. This peculiarity of double detachment is due to the high ratio of ionization potential to electron affinity of atoms. It demonstrates the possibility of studying strong-field ionization of atoms prepared by means of photodetachment. Our results suggest that for the study of nonsequential detachment application of laser pulses much shorter than 100 fs is required in order to overcome the saturation regime.

The authors greatly appreciate fruitful discussions with Professor Hanspeter Helm. This research is supported by the Deutsche Forschungsgemeinschaft, Grant No. KI 865/1-3.

[1] N. B. Delone and V. P. Krainov, *Multiphoton Processes in Atoms* (Springer-Verlag, Berlin, 2000).
[2] L. F. Di Mauro and P. Agostini, Adv. At. Mol. Opt. Phys. **35**, 79 (1995).
[3] B. Walker *et al.*, Phys. Rev. Lett. **73**, 1227 (1994).
[4] A. Becker and F. H. M. Faisal, Phys. Rev. A **59**, R1742 (1999).
[5] Th. Weber *et al.*, Phys. Rev. Lett. **84**, 443 (2000); J. Phys. B **33**, L127 (2000).
[6] R. Moshammer *et al.*, Phys. Rev. Lett. **84**, 447 (2000).
[7] P. B. Corkum, Phys. Rev. Lett. **71**, 1994 (1993).
[8] A. Rudenko *et al.*, Phys. Rev. Lett. **93**, 253001 (2004).
[9] J. B. Greenwood *et al.*, J. Phys. B **36**, L235 (2003).
[10] J. Pedregosa-Gutierrez *et al.*, Phys. Rev. Lett. **93**, 223001 (2004).
[11] H. W. van der Hart, Phys. Rev. A **74**, 053406 (2006).
[12] B. Bergues *et al.*, Phys. Rev. A **75**, 063415 (2007).
[13] G. F. Gribakin and M. Yu. Kuchiev, Phys. Rev. A **55**, 3760 (1997).
[14] H. R. Reiss, Prog. Quantum Electron. **16**, 1 (1992).
[15] M. V. Ammosov, N. B. Delone, and V. P. Krainov, Sov. Phys. JETP **64**, 1191 (1986).